Reconfigurable Type I and Type II Buck-Boost Partial Power Converter for EV Fast Chargers

Pesantez, Daniel; Renaudineau, Hugues; Kouro, Samir; Rivera, Sebastian; Rodriguez, Jose

DOI
10.1109/PEDES61459.2024.10960851

Publication date
2024

Document Version
Final published version

Published in
Proceedings of the 2024 IEEE International Conference on Power Electronics, Drives and Energy Systems (PEDES)

Citation (APA)
Pesantez, D., Renaudineau, H., Kouro, S., Rivera, S., & Rodriguez, J. (2024). Reconfigurable Type I and Type II Buck-Boost Partial Power Converter for EV Fast Chargers. In *Proceedings of the 2024 IEEE International Conference on Power Electronics, Drives and Energy Systems (PEDES)* (2024 ed.). (Proceedings of the International Conference on Power Electronics, Drives, and Energy Systems for Industrial Growth, PEDES). IEEE. https://doi.org/10.1109/PEDES61459.2024.10960851

Reconfigurable Type I and Type II buck-boost partial power converter for EV fast chargers

Daniel Pesantez
Centro de Transición Energética, Facultad de Ingeniería, Arquitectura y Diseño, Universidad San Sebastián
Santiago, Chile
alvaro.pesantez@sansano.usm.cl

Hugues Renaudineau
Department of Electronic Engineering Univ. Tecnica Federico Santa Maria
Valparaiso, Chile
hugues.renaudineau@usm.cl

Samir Kouro
Department of Electronic Engineering Univ. Tecnica Federico Santa Maria
Valparaiso, Chile
samir.kouro@ieee.org

Sebastian Rivera
DCE&S Group
Department of Electrical Sustainable Energy
Delft University of Technology
Delft, The Netherlands
s.rivera.i@ieee.org

Jose Rodriguez
Centro de Transición Energética, Facultad de Ingeniería, Arquitectura y Diseño, Universidad San Sebastián
Santiago, Chile
jose.rodriguezp@uss.cl

2024 IEEE International Conference on Power Electronics, Drives and Energy Systems (PEDES) | 979-8-3503-7247-2/24/$31.00 ©2024 IEEE | DOI: 10.1109/PEDES61459.2024.10960851

***Abstract*—This work introduces a reconfigurable topology for AC-link partial power converters (PPC), intended for use as high-frequency transformerless regulated DC-DC converters in fast charging stations for electric vehicles (EV). This new topology allows an AC-link PPC to be reconfigured so that it works as a type I PPC during boost mode and as a type II PPC during buck mode. The converter is able to operate across a wide output voltage range, making it compatible with the different battery voltage configurations found in the electric vehicle industry. The converter is reconfigured using four additional switches. Depending on the operating mode, these switches can be turned on or off to achieve the desired topology. In a type I PPC configuration, the input is connected in parallel, and the output is connected in series with the battery. In a type II configuration, the input is connected in series, and the output is connected in parallel with the battery. This paper presents an analysis of converter operations and control for EV charging systems operating at 400 V and 800 V, incorporating both operation validation and efficiency metrics derived from simulations.**

***Index Terms*—Electric vehicles, fast chargers, partial power converters.**

I. Introduction

The ongoing progress in the electric vehicle (EV) sector is closely linked with advancements in battery technology. Advances in battery technology have led to improvements such as higher capacity and extended lifespan, enabling electric vehicles to achieve greater autonomy and range, making them more attractive to consumers. In the early stages of growth of the EV industry, battery setups with voltages ranging from 150 V to 450 V were commonly employed, with some researchers categorizing these as 400 V systems. However, in recent years, to increase the EV power density, efficiency, and charging power rate to reduce charging times, battery configurations have been developed to increase their voltage. The latest power-trains exhibit voltages in the range between 700 V to 900 V, commonly referred to as 800 V systems [1].

This has led to the coexistence of both battery voltage systems, posing an additional challenge for EV battery chargers. Therefore latest chargers must not only regulate the current injected into the battery using a suitable charging algorithm, improve power conversion efficiency, and decrease charging times, but also manage a wider output voltage range [2], [3]. In the existing literature, various types of chargers are available for charging 400 V and 800 V battery systems. For instance, an integrated reconfigurable converter topology for high-voltage battery systems is proposed in [4]. However, this converter operates by reconfiguring both the battery and the battery management system (BMS), resulting in a solution that is both expensive and complex to implement. In [5], solutions are discussed that adapt chargers originally designed for 400 V systems by using a battery selection circuit. However, these configurations have a restricted charging range and do not support batteries with nominal voltages that differ significantly from 400 V or 800 V. The main challenge for wide-output voltage range chargers is to perform with similar efficiency across the voltage range.

On the other hand, Partial Power Converters (PPC) have emerged recently as a promising alternative for the DC-DC stage of battery chargers, due to the high efficiency they offer. A key characteristic of these converters is their ability to process just a fraction of the total power supplied to the battery, with the remaining power being directly transferred through a bypass in some operating states. By dealing with only a fraction of the power, the conduction and switching losses of the converter are reduced, which improves the overall converter efficiency [6]. In the literature, PPCs are primarily categorized based on their connection method to the remainder of the system. Among the various configurations, two setups are of particular interest for EV battery charging applications, namely the input-parallel output-series (IPOS) and input-series output-parallel (ISOP) topologies. The IPOS step-up topology is known as Type I PPC, while the ISOP step-down topology is referred to as Type II PPC [6], [7].

This work introduces a reconfigurable DC-DC PPC with a wide output voltage range. The converter can adapt its operation based on the connected battery system. It functions as a Type I PPC, for 800 V battery systems, and as a Type II PPC for 400 V battery systems. Section II provides an analysis of the proposed reconfigurable PPC. In Section III, the simulation results for the converter operating in an EV battery charging scenario for both 400V and 800V systems are detailed. Finally, Section IV summarizes the conclusions of the work. The following sections present the reconfigurable converter and some simulation results.

II. Proposed Converter

Generic block diagrams for Type I and Type II PPCs are illustrated in Fig. 1. It is important to note that a PPC includes a full power converter (FPC), rated at lower capacity than the charger, embedded within the power circuit. However, its input or output connection to the rest of the charging system enables the processing of only a fraction of the total power supplied to the battery. In Fig.1, P_{pc} represents the power handled by the FPC, P_{dir} represents the power that goes directly to the battery, hence $P_o = P_{pc} + P_{dir}$ represents the total power delivered to the battery. The voltage withstood by the converter is denoted as V_{pc}, while the input and output voltage of the DC-DC regulation stage are represented by V_{in} and V_o, respectively.

Type I PPC configurations are primarily used in voltage-step-up charging systems. This is due to their ability to function with a partiality factor, defined as the ratio of the power managed by the converter P_{PC} to the input power P_{in}, for any converter output-input voltage ratio exceeding 1. For converter voltage ratios below 1, Type I converters operate as PPCs within a restricted range. In contrast, Type II PPCs are employed in voltage-step-down charging systems. This is because their PPC operating ratio is constrained for converter gain values greater than 1, whereas for values lower than 1, they function as PPCs without limitations. A comprehensive examination of these characteristics of Type I and Type II PPCs can be found in [6], [7].

To combine the benefits of type I and type II PPCs into a unified topology that allows the converter to be reconfigured according to the system requirements, in [8] a reconfigurable PPC topology is proposed as power optimizer for photovoltaic grid-connected systems. This reconfiguration concept, illustrated in Fig. 2, enables the converter to function as a Type I PPC when switches S_{U1} and S_{U2} are closed and switches S_{D1} and S_{D2} are open. In contrast, when switches S_{U1} and S_{U2} are open and switches S_{D1} and S_{D2} are closed, the converter operates as a Type II PPC. Applying the same reconfiguration

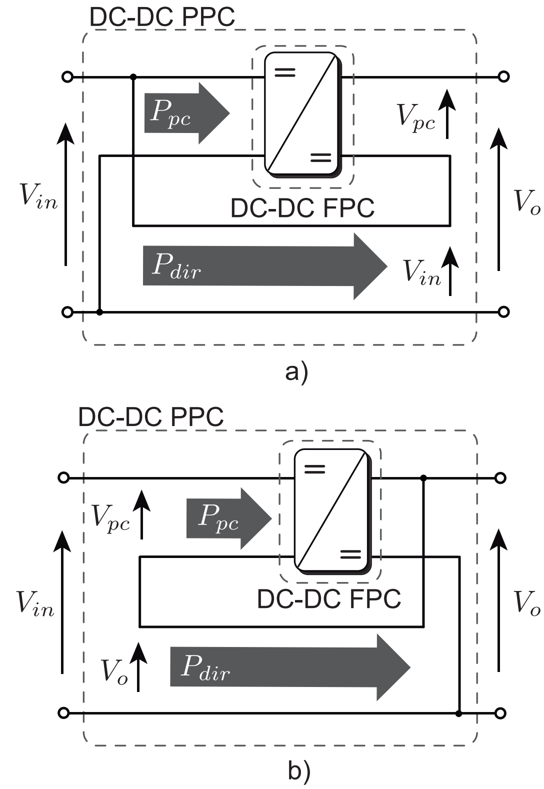

Fig. 1. General structure of a DC-DC PPC: a) Type I PPC; b) Type II PPC.

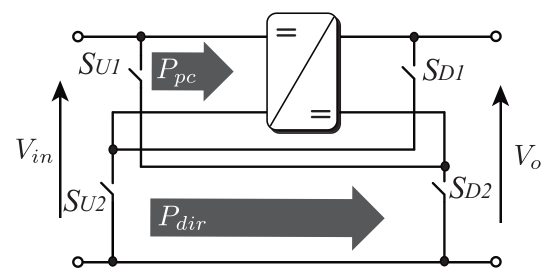

Fig. 2. Generic circuit topology of the proposed reconfigurable PPC.

principle, using the Type I AC-link impedance network PPC described in [6], along with the Type II variant of the converter in [9], results in the proposed reconfigurable Type I and Type II buck-boost PPC for EV fast chargers shown in Fig. 3.

The switches S_{U1}, S_{U2}, S_{D1}, and S_{D2} enable the system to be reconfigured based on the logic outlined previously. In the scenario where the converter operates in boost mode [6], meaning it is set up as a Type I PPC, as shown in Fig. 4 a), the converter employs a full-bridge configuration at the input and a diode-bridge in series with the output, generating a series voltage between the input DC-link and the battery. Based on the switching state of the semiconductors S_a, S_b, S_c and S_d, the voltage across capacitors C_1 or C_2 is connected in series with the input voltage and the inductive output filter L. In buck mode operation, with the converter set up as a Type II

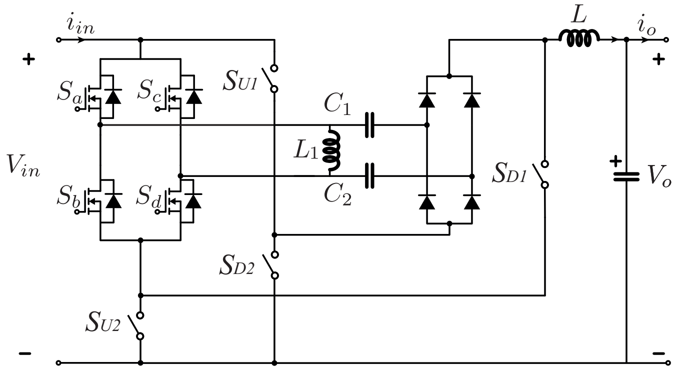

Fig. 3. Reconfigurable type I and type II buck-boost PPC based on CLC AC-link.

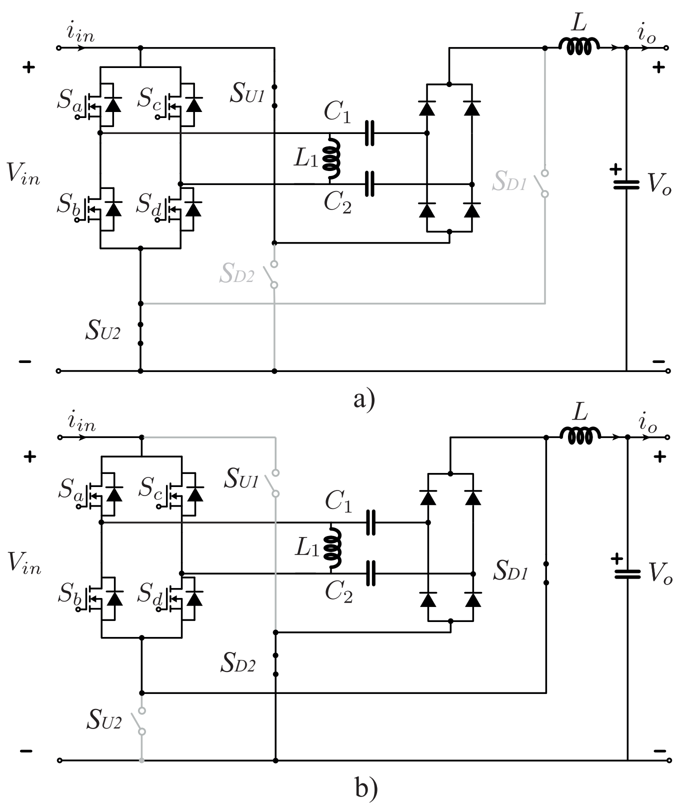

Fig. 4. Proposed reconfigurable PPC: a) Type I boost-mode PPC. b) Type II buck-mode PPC.

PPC, as shown in Fig. 4 b), the input full-bridge is connected to the diode full-bridge, which is connected in parallel with the battery. In both configurations, the connection between the input full-bridge and the diode-bridge is connected through an AC-link composed of capacitors C_1, C_2, and inductor L_1.

For the Type I reconfigurable converter shown in Fig. 4 a), and given that T and α represent a switching period and the phase-shift angles between the control signals of the switches S_a, S_b, S_c and S_d, the equations for the state variables are:

1) Switching state I: (S_a, S_c) = (1, 0):

$$\begin{aligned} L_1\frac{di_1}{dt} &= V_{in} \\ V_{C_2} &= V_{in} \\ C_1\frac{dV_{C_1}}{dt} &= -i_L \\ L\frac{di_L}{dt} &= V_{in} + V_{C_1} - V_o \\ C_o\frac{dV_o}{dt} &= i_L - i_o \end{aligned} \tag{1}$$

2) Switching state II: (S_a, S_c) = (1, 1):

$$\begin{aligned} L_1\frac{di_1}{dt} &= 0 \\ V_{C_1} &= V_{C_2}, \\ C_1\frac{dV_{C_1}}{dt} + C_2\frac{dV_{C_2}}{dt} &= -i_L \\ L\frac{di_L}{dt} &= V_{in} + V_{C_1} - V_o \\ C_o\frac{dV_o}{dt} &= i_L - i_o \end{aligned} \tag{2}$$

3) Switching state III: (S_a, S_c) = (0, 1):

$$\begin{aligned} L_1\frac{di_1}{dt} &= -V_{in} \\ V_{C_1} &= V_{in} \\ C_2\frac{dV_{C_2}}{dt} &= -i_L \\ L\frac{di_L}{dt} &= V_{in} + V_{C_2} - V_o \\ C_o\frac{dV_o}{dt} &= i_L - i_o \end{aligned} \tag{3}$$

4) Switching state IV: (S_a, S_c) = (0, 0):

$$\begin{aligned} L_1\frac{di_1}{dt} &= 0 \\ V_{C_1} &= V_{in} \\ V_{C_2} &= V_{in} \\ L\frac{di_L}{dt} &= V_{in} - V_o \\ C_o\frac{dV_o}{dt} &= i_L - i_o \end{aligned} \tag{4}$$

For the Type II reconfigurable converter shown in Fig. 4 b), the equations for the state variables are:

5) Switching state V: (S_a, S_c) = (1, 0):

$$\begin{aligned} V_{C_2} &= L_1\frac{di_{L_1}}{dt} \\ L\frac{di_L}{dt} &= V_{in} + V_{C_1} - V_o \\ C_o\frac{dV_o}{dt} &= i_L - i_o \end{aligned} \tag{5}$$

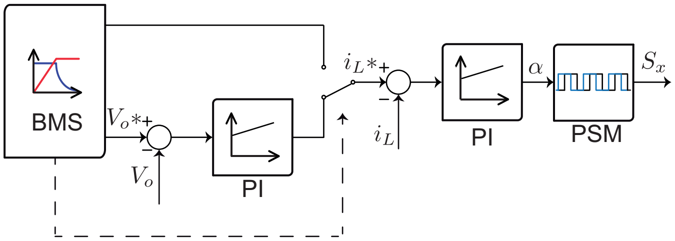

Fig. 5. CC-CV control scheme.

6) Switching state VI: (S_a, S_c) = (1, 1):

$$\begin{aligned} V_{C_2} &= V_{C_1} \\ L\frac{di_L}{dt} &= V_{in} + V_{C_1} - V_o \\ C_o\frac{dV_o}{dt} &= i_L - i_o \end{aligned} \tag{6}$$

7) Switching state VII: (S_a, S_c) = (0, 1):

$$\begin{aligned} V_{C_1} &= L_1\frac{di_{L_1}}{dt} \\ L\frac{di_L}{dt} &= V_{in} + V_{C_2} - V_o \\ C_o\frac{dV_o}{dt} &= i_L - i_o \end{aligned} \tag{7}$$

8) Switching state VIII: (S_a, S_c) = (0, 0):

$$\begin{aligned} V_{C_1} &= V_{C_2} \\ L\frac{di_L}{dt} &= V_{C_1} - V_o \\ C_o\frac{dV_o}{dt} &= i_L - i_o \end{aligned} \tag{8}$$

For a detailed examination of the mathematical model of the converter that functions as Type I or Type II, refer to [6], [9], which illustrates the method used to derive the transfer function used in the design of the converter control parameters.

III. Simulation Results

To regulate the battery charge process, the Constant-Current and Constant-Voltage (CC-CV) algorithm is used [10]. This algorithm consists of two stages. In the initial stage, known as constant current, the battery is charged with a constant current, the nominal value is set by the manufacturer defining the capacity of the charger. In the second stage, known as constant voltage, the battery is not overcharging by limiting the current flowing into it, allowing the battery to achieve a full battery charge in a regulated way.

The reconfigurable PPC control is implemented through a cascaded control of two PI control loops, one internal current control with faster dynamics and one external voltage control with slower dynamics, shown in Fig.5, In this context, V_O^* denotes the voltage reference, which corresponds to the nominal battery voltage, I_L^* indicates the current reference, and α signifies the phase shift angle between the output signals of the Phase Shift Modulation (PSM) block. The internal current controller receives its reference directly from the BMS during the CC charge state, maintaining a constant value. However, once the battery reaches a specific State of Charge (SoC), the reference shifts to the output of the external voltage controller, which ensures that the battery achieves its maximum voltage level in a controlled way, preventing any battery overload.

To test the topology, the charging process for battery systems of 400 V and 800 V is considered. Table I shows the parameters used to simulate the DC-DC converter as part of the fast charging station. For both systems, the input voltage is considered to be equal to 500 V.

Fig. 6 presents the simulation results for the converter that operates as a Type II PPC with a 400 V battery configuration. A 60 kWh battery, with a nominal voltage of 410 V and an

Table I
Simulation Parameters

Parameter	400 V System	800 V System
Input Voltage	500 V	500 V
CC mode	100 A	100 A
Output Inductor	180 uH	180 uH
L1 Inductor	10 uH	10 uH
C_1 and C_2 Capacitors	100 uF	100 uF
Switching Frequency	20 kHz	20 kHz

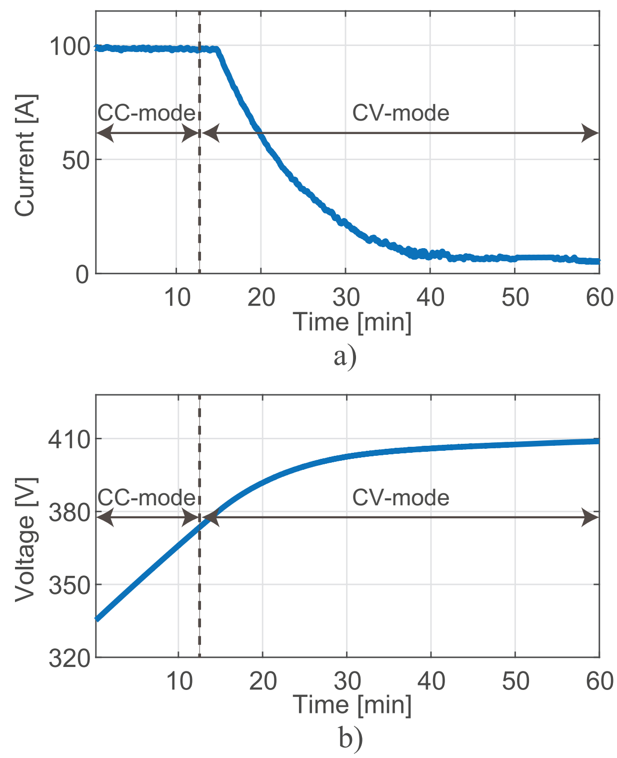

Fig. 6. Simulation results for Type II PPC operation for 400V system: a) Output current, b) Output voltage.

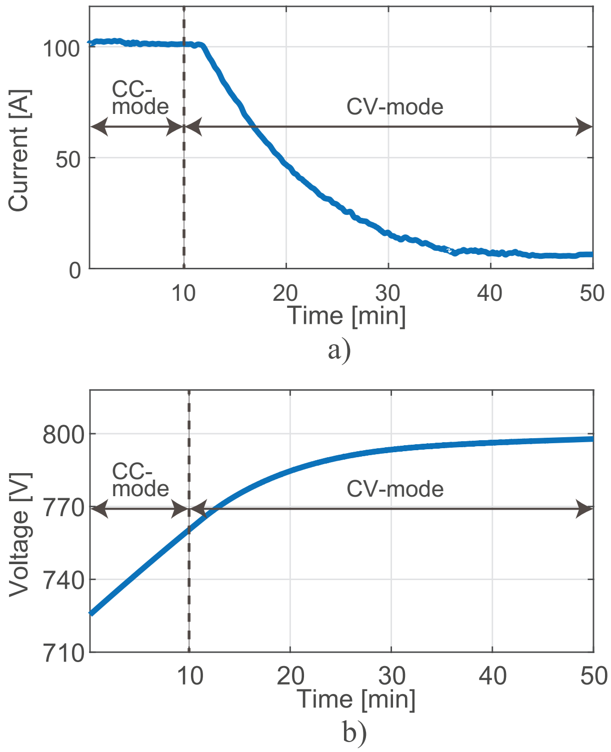

Fig. 7. Simulation results for Type I PPC operation for 800V system: a) Output current, b) Output voltage.

initial SoC of 20%, is charged using the CC-CV algorithm. Initially, a constant current of 100 A is applied for about 13 minutes until the battery reaches an SoC of 80%. At this point, the control algorithm switches to CV mode, allowing the battery to dictate the current required to complete the charge. The battery is fully charged in approximately 50 minutes.

Fig. 7 shows the charging procedure for a battery with a nominal voltage of 800 V and an initial SoC of 20%, using a Type I PPC configuration. Initially, the battery is fed a current of 100 A during the CC stage. Around the 10-minute mark, the battery reaches an 80% SoC and transitions to CV mode. These figures show how the current decreases as the battery voltage increases, nearing its nominal value, ensuring a safe full charge. The entire process takes approximately 40 minutes.

In Fig. 8, the efficiency analysis for the proposed converter is presented. This analysis was conducted using the thermal model of the semiconductors using the PLECS software, employing the C3M0025065D MOSFET and the GD2X20MPS12D diode. The simulation covered the two proposed converter configurations within the same power range, from 1 kW to 10 kW. For the converter operating as PPC type I (shown by the red curve), the peak efficiency of 97.9% was achieved at 10 kW. Meanwhile, for the converter operating as PPC type II (indicated by the blue curve), a maximum efficiency of 98.8% was reached, also at 10 kW.

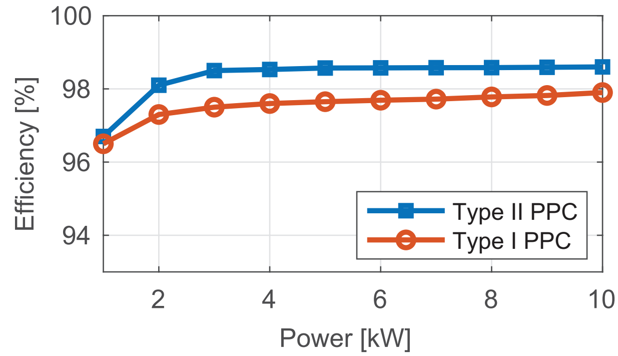

Fig. 8. Efficiency simulation results.

IV. Conclusions

This work introduces a reconfigurable Type I and Type II buck-boost PPC, designed for use as the DC-DC converter in fast charging stations. With its wide output voltage range, it enables charging stations to accommodate EVs with both 400V and 800V battery systems. Simulation results demonstrate the proper functioning of the proposed converter and control during an electric vehicle fast charging process. The converter operating principle with the corresponding switching states, equations, and dynamic model was presented. Furthermore, an efficiency analysis demonstrated that the converter can achieve high efficiency levels, a characteristic of partial power converters. The peak efficiency was observed when the converter operates as a type II PPC, in step-down mode, reaching a maximum of 98.9%. The notable efficiency and capability to manage a wide output voltage range make this converter an excellent candidate for EV battery charging applications. It can also be easily adopted in charging architectures that feature low-frequency galvanic isolation since no galvanic isolation is included in the proposed PPC topology. If used for high-frequency isolation architectures, the proposed converter can be combined with an unregulated DC-DC conversion stage with high-frequency galvanic isolation, such as a DCX converter, since the proposed PPC can perform the battery charging process regulation.

Acknowledgment

This work was supported in part by ANID under grant Fondecyt 1221741, AC3E (ANID/Basal/FB0008), SERC Chile (ANID/Fondap/1523A0006), and Doctorado Nacional/2022/21221405.

References

[1] C. Jung, “Power Up with 800-V Systems: The benefits of upgrading voltage power for battery-electric passenger vehicles,” *IEEE Electrification Magazine*, vol. 5, no. 1, pp. 53–58, 2017.

[2] A. Elezab, O. Zayed, A. Abuelnaga, and M. Narimani, “High Efficiency LLC Resonant Converter With Wide Output Range of 200-1000 V for DC-Connected EVs Ultra-Fast Charging Stations,” *IEEE Access*, vol. 11, no. April, pp. 33 037–33 048, 2023.

[3] H. Karneddi and D. Ronanki, “Universal Bridgeless Nonisolated Battery Charger With Wide-Output Voltage Range,” *IEEE Transactions on Power Electronics*, vol. 38, no. 3, pp. 2816–2820, 2023.
[4] M. Momayyezan, B. Hredzak, and V. G. Agelidis, “Integrated Reconfigurable Converter Topology for High-Voltage Battery Systems,” *IEEE Transactions on Power Electronics*, vol. 31, no. 3, pp. 1968–1979, 2016.
[5] J. Y. Kim, B. S. Lee, D. H. Kwon, D. W. Lee, and J. K. Kim, “Low Voltage Charging Technique for Electric Vehicles with 800 v Battery,” *IEEE Transactions on Industrial Electronics*, vol. 69, no. 8, pp. 7890–7896, 2022.
[6] D. Pesantez, H. Renaudineau, S. Rivera, A. Peralta, A. Marquez Alcaide, and S. Kouro, “Transformerless partial power converter topology for electric vehicle fast charge,” *IET Power Electronics*, vol. 17, no. 8, pp. 970–982, 2024.
[7] S. Rivera, J. Rojas, S. Kouro, P. W. Lehn, R. Lizana, H. Renaudineau, and T. Dragicevic, “Partial-Power Converter Topology of Type II for Efficient Electric Vehicle Fast Charging,” *IEEE Journal of Emerging and Selected Topics in Power Electronics*, vol. 10, no. 6, pp. 7839–7848, 2022.
[8] H. Renaudineau, D. Pesantez, N. Muller, F. Flores-Bahamonde, S. Kouro, and J. Rodriguez, “Reconfigurable step-up/down partial power converter for PV power optimizer,” *2022 IEEE Energy Conversion Congress and Exposition, ECCE 2022*, pp. 1–6, 2022.
[9] E. Richard, H. Renaudineau, A. M. Llor, R. A. Bugueno, and C. A. Rojas, “Transformerless Partial Power AC-Link Converter for PV Integration to DC Microgrid,” *IECON Proceedings (Industrial Electronics Conference)*, vol. 2022-Octob, 2022.
[10] W. Shen, T. T. Vo, and A. Kapoor, “Charging algorithms of lithium-ion batteries: An overview,” *Proceedings of the 2012 7th IEEE Conference on Industrial Electronics and Applications, ICIEA 2012*, pp. 1567–1572, 2012.